

Temporary Well Plugging for Future CO₂ Storage: CT Analysis of Thermal Sensitive Polymer-Gel Dynamics in Low-Permeability Chalk

Hamed Movahedi¹, Adrian A. Schiefler¹, Sumant Dwivedi², Henning Osholm Sørensen³, Henning-Friis Poulsen¹, Nicolas Bovet⁴

¹Department of Physics, Technical University of Denmark
Fysikvej, 2800 Kgs. Lyngby, Copenhagen, Denmark
hammo@dtu.dk; aalsc@dtu.dk; hfpo@fysik.dtu.dk

²School of Polymer Science and Engineering, The University of Southern Mississippi
Hattiesburg, MS 39406, USA
supernalsumant@gmail.com

³Xnovo Technology
ApS, Galoche Alle 15, 1., Køge, DK-4600, Denmark
osho@fysik.dtu.dk

⁴Danish Offshore Technology Centre, Technical University of Denmark
Elektrovej 375DK-2800 Kgs. Lyngby, Copenhagen, Denmark
nbovet@dtu.dk

Abstract – Since most oil and gas reservoirs are nearing the end of their productive lifespans, environmental regulations require wells to be securely plugged before they are abandoned to reduce pollution hazards. This study investigates the use of polymer gels for temporary *in-situ* plugging in chalk formations with low permeability, a challenging environment since high-viscosity fluid injection is problematic. First, a cross-linker and polymer combination with low viscosity are injected into the chalk matrix inside a core holder. Subsequently, when heated this combination forms a gel, significantly raising the viscosity, and effectively blocking the flow channels in the porous medium. Real-time monitoring using computed tomography (CT) analysis is used to verify the plugging procedure and ensure the polymer is injected evenly. Flow tests are performed after gelation to evaluate the level of permeability. The study is expanded to include fractured media to assess how effectively the gel blocks matrix porosity as well as fractures. The findings provide insight on well-plugging methods that support these wells' conversion to CO₂ storage locations, with potential benefits for improving operational sustainability and environmental safety.

Keywords: Oil Well Abandonment, Porous Media Sealing, Polymer Gel, Computed Tomography

1. Introduction

The utilization of hydrocarbon and fossil fuel resources had a significant surge throughout the industrial revolution, thus prompting a growing focus on sustainable methodologies aimed at mitigating carbon emissions and promoting the adoption of renewable energy sources [1]. Conversely, there is now a global energy transition underway, characterized by a concerted effort to adopt renewable and ecologically sustainable energy sources. This shift has led to increased number of regulations on the extraction and utilization of oil and gas, including an emphasis on the need of plugging and abandonment procedures. In the context of wellbore integrity, cement plugs are commonly employed at various intervals to ensure adequate plugging. Nevertheless, other factors might pose significant obstacles to the long-term resilience of cement, including the conditions within the wellbore, the presence of fissures, and suboptimal execution of cement procedures [2-4].

In wellbore abandonment and plugging, several materials are used depending on well conditions and position (Table 1). To determine whether a well barrier is suitable for its intended purpose, it is important to fulfil certain requirements known as Well Barrier Acceptance Criteria (WBAC). These requirements encompass both functional and verification aspects of the well barrier. The primary functional qualities that permanent barrier materials must possess include having very low permeability or being impermeable, exhibiting long-term durability under downhole conditions, not shrinking, being ductile or non-brittle, being able to resist downhole fluids and gases, and having sufficient bonding to the formation [5-7]. In the Danish sector of the North Sea, a significant environmental challenge arises from the necessity to install cement plugs within

wellbores lined with hazardous scales, where any mechanical intervention during this process heightens the risk of contamination. Polymer gels have already been used in several water conformance projects and plugging high-perm zones during water flooding. Various types of monomers which have been used to make polymer gels are shown in Fig. 1. Among them, acrylamide (AM) is one of the most popular, as it can be synthesized as a partial hydrolysed and anionic polymer for use as viscosifier or gelation agent [8-12]. In this work, polyacrylamide was synthesized and modified by Hoffman rearrangement followed by adding the Glutaraldehyde crosslinker to the solution at constant value. The solution underwent gelation at the reservoir temperature (60-80°C) upon heating. Prior to injection, a numerical simulation was done on a flow cell (core holder) to determine the flow rate at which the temperature remains at the desired value for gel formation.

Table 1: Materials used for well plugging [5].

Type	Material	Example
A	Cements	Portland cement, pozzolanic cements, slag, and geopolymers
B	Grouts	Sand or clay mixture, barite plugs, and calcium carbonate
C	Thermosetting polymers	Resins, epoxy, and polyester
D	Thermoplastic polymers	Polyethylene, polypropylene, polyamide, and polycarbonate
E	Elastomeric polymers	Natural rubber, neoprene, nitrile, silicone rubber, and polyurethane
F	Formation	Claystone, shale, and salt
G	Gels	Polymer gels, polysaccharides, starches, and silicate base gels
H	Metals	Steel, Aluminium

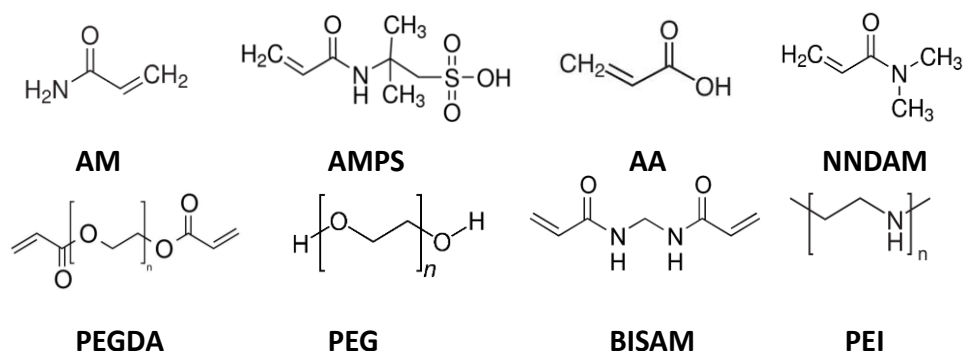


Fig. 1: Various monomers utilized in the synthesis of polymer gels for petroleum industry applications.

2. Experiment and Methods

2.1. Synthesis and Flow Setup

Polyacrylamide was synthesized by free radical polymerization, followed by partial amination to improve cross-linking activity. The amine-modified polyacrylamide that results has enhanced reactivity with glutaraldehyde, generating a heat-induced gel that might be used as a plugging agent. In the context of this study, cylindrical chalk core samples (see table 2) obtained from Danish oil reservoirs were used to evaluate plugging performance.

To apply lithostatic pressures to the chalk samples, a custom-fabricated core holder flow cell was used. This was designed to resemble *in situ* stress and to comply with underground pressure conditions. Moreover, it allowed for the precise control of fluid dynamics, such as injection rates and pressures, in a setting similar to those seen in petroleum extraction wells. The core holder was fitted with a thermal jacket to simulate the thermal environment of oil reservoirs, giving temperature control realistic of deep geological conditions. Fig. 2 depicts the experimental setup, illustrating the core holder mechanism.

Table 2: Properties and dimensions of chalk core plugs used in this study.

Sample No.	Core status	Length(cm)	Diameter(cm)	Matrix Porosity
1	Fractured	2	2.54	0.29
2	Unfractured	4.4	2.54	0.31

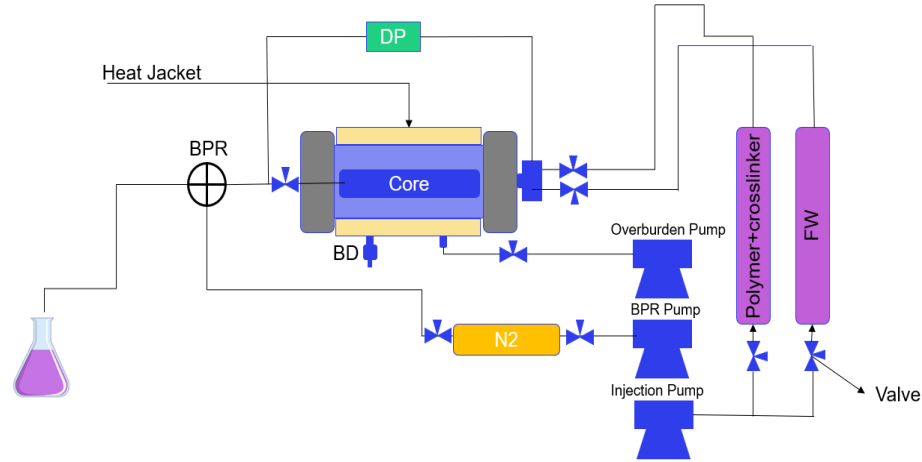


Fig. 2: Core flooding system

2.2. X-Ray Tomography Setup

X-ray microcomputed tomography offers a promising and non-destructive method for acquiring detailed information about the internal dynamics of porous media during the injection of various fluids [13,14]. The polymer injection and gelation processes within the chalk were monitored using a Nikon XT CT scanner at the 3D Imaging Center at DTU. The micro-focus X-ray tube was operated at 155 kV for ex-situ scans and at 215 kV for in-situ CT scans. Projection images were captured either with 1×1 binning, yielding an effective pixel size $14.38 \mu\text{m}$ and 2000×2000 pixels, or with 2×2 binning yielding an effective pixel size of $62 \mu\text{m}$ and 1000×1000 pixels. The exposure time for each image varied between 1.4 and 2.83 seconds. To ensure the projections fit within the field of view of the detector, the distance between the source and detector was maintained consistently. The 360 deg rotation was executed in 1571 steps.

2.2. Numerical Simulation of Heat Transfer in Porous Media

To achieve a homogenous thermal distribution within the porous medium during injection operations, it is crucial to administer the fluid at a flow rate that permits adequate heat uptake from the surroundings. High flow rates can impede thermal equilibrium, as the fluid may not assimilate sufficient heat from the core holder's exterior. To address this issue, two-dimensional simulations of fluid flow coupled with heat transfer were conducted using COMSOL Multiphysics software.

Within the simulations, the core holder's central region, containing the cylindrical core, was modeled as a porous medium. Surrounding this core, the interstitial space, filled with water, was treated as a continuum. The outer shell was defined as a solid in the model. Darcy's law was applied to describe the flow within the porous media, with the flow dynamics being directly coupled to heat transfer equations. Convective heat transfer was assumed to dominate at the fluid's free-flow boundaries and in the interaction between the core rock and the water in the surrounding annulus. In contrast, conductive heat transfer was presumed to be the primary mechanism of thermal energy exchange within the solid components of the system.

3. Results and Discussion

Fig. 3 illustrates the temperature profiles within the chalk core, the fluid shell around it, and the aluminium body of the core holder. During the experiment, water at an initial temperature of 25°C , was introduced into the chalk, which possessed a porosity value of 0.31. The injection of water occurred at two distinct flow rates: 1 cc/min and 0.1 cc/min. This process

was carried out continuously for a total period of 100 minutes. Concurrently, the external aluminum casing of the core holder was consistently maintained at a temperature of 80°C. The graphic clearly demonstrates that the temperature distribution within the core becomes non-uniform as the flow rates increase. The lack of homogeneity has significance when considering experimental design, as the flow transport in this setting exhibits reactivity and temperature dependence.

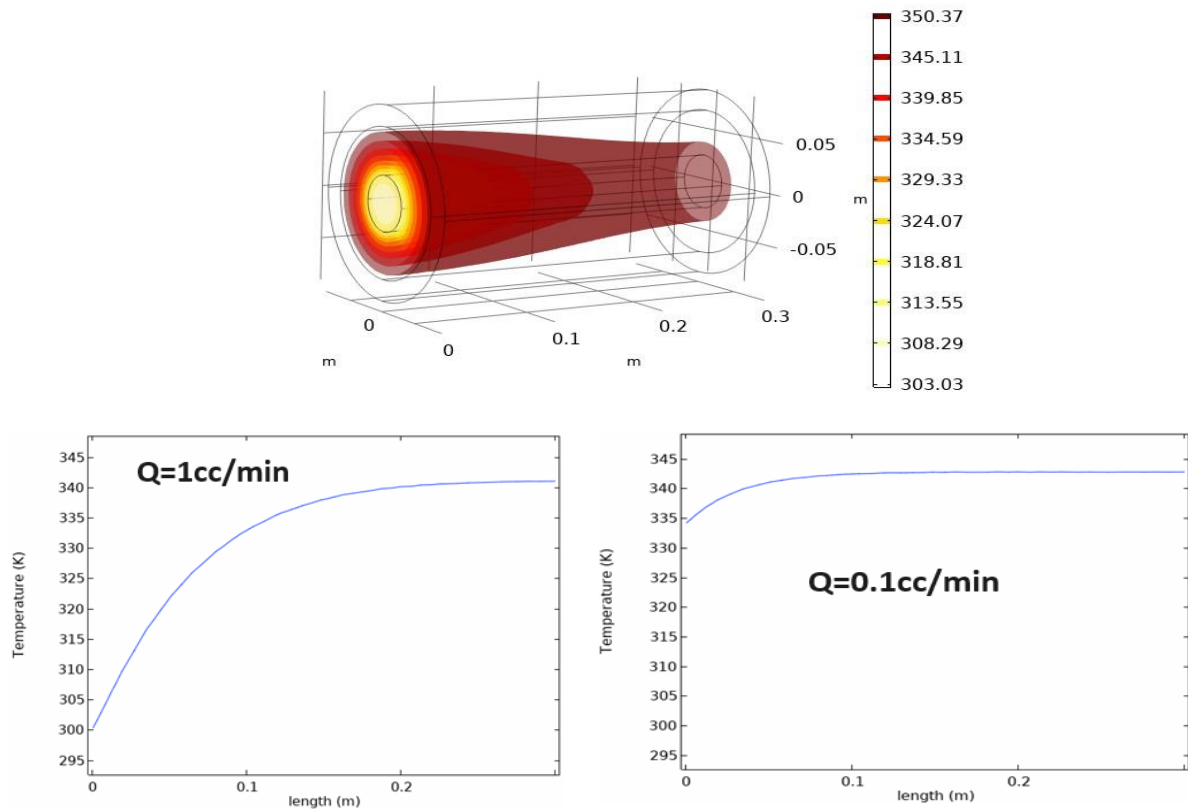


Fig. 3: Three-dimensional isosurface temperature distribution within the core holder containing a chalk sample with the inlet to the left and with $Q=1\text{cc/min}$. Below: the temperature profile along the center line of the cylindrical sample.

Fig. 4 presents the rheological properties of the polymer solution and the gelation time when combined with a crosslinker. The figure demonstrates that the polymer solution exhibits non-Newtonian, power-law fluid behavior, characterized by a decrease in viscosity with an increase in shear rate. Additionally, the gelation time is shown to be dependent on the polymer concentration, with higher concentrations leading to quicker gelation. All gel time tests were conducted at a constant temperature of 80°C.

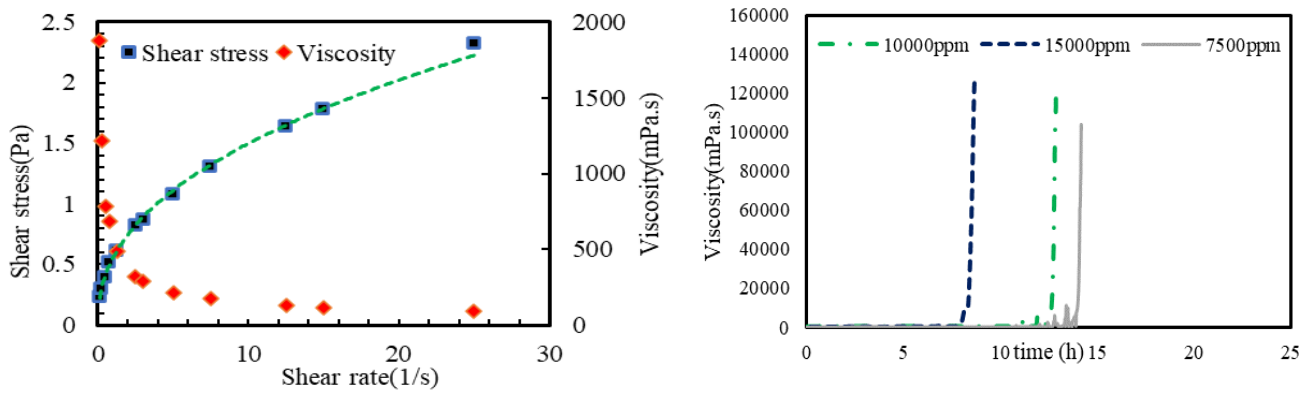


Fig. 4: Rheological behavior (left) and gel time for polymer at different concentrations (right).

Fig. 5 displays CT images of a fractured chalk core rock, captured from various planar views (sections). This image vividly illustrates the fracture aperture and orientation, which are discernible due to the application of segmentation and thresholding analyses. Subsequently, dynamic CT imaging was conducted to observe real-time fluid flow through the chalk contained within a core holder. These images, taken at different time intervals, effectively demonstrate the dispersion patterns of the polymer and base fluid.

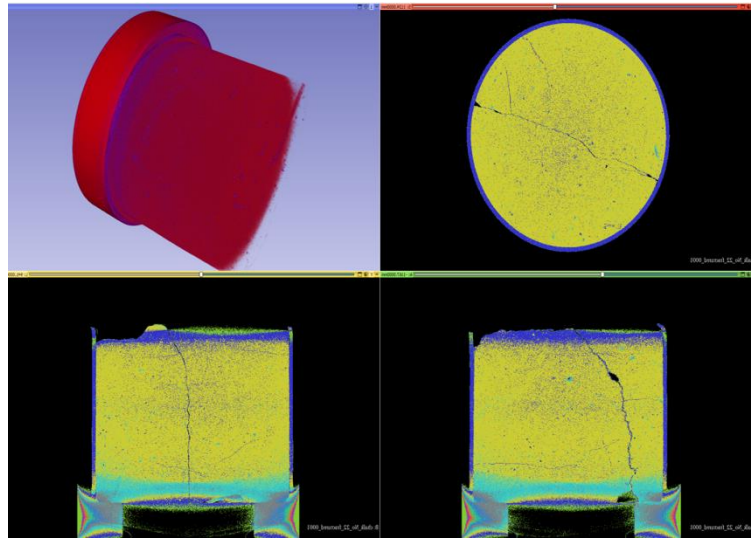


Fig. 5: CT scan of a fractured chalk sample (without contrast agent and before polymer injection). Four slices through the reconstructed 3D volumes are shown, representing different view angles.

Figure 6 displays the dynamic computed tomography (CT) scan of fractured chalk during the process of injecting polymer with initial concentration of 4000 ppm into the porous media. Prior to the introduction of polymer injection, the chalk was saturated with a suitable contrast agent, CsCl, to increase the absorption of X-ray photons and thus improve the contrast in the images. The initial set of images shows the intensity distribution of subtracted projections, highlighting contrast differences between non-saturated and CsCl-saturated chalk. Notably, fractures become visible as distinct, brighter lines in the third image. Following this, polymer gel is introduced, displacing the contrast agent-saturated fluid, which is

reflected in increased brightness in subsequent images. The differentiation between CsCl-saturated and polymer-saturated images at each time step allows for clear visualization of the advancing polymer front.

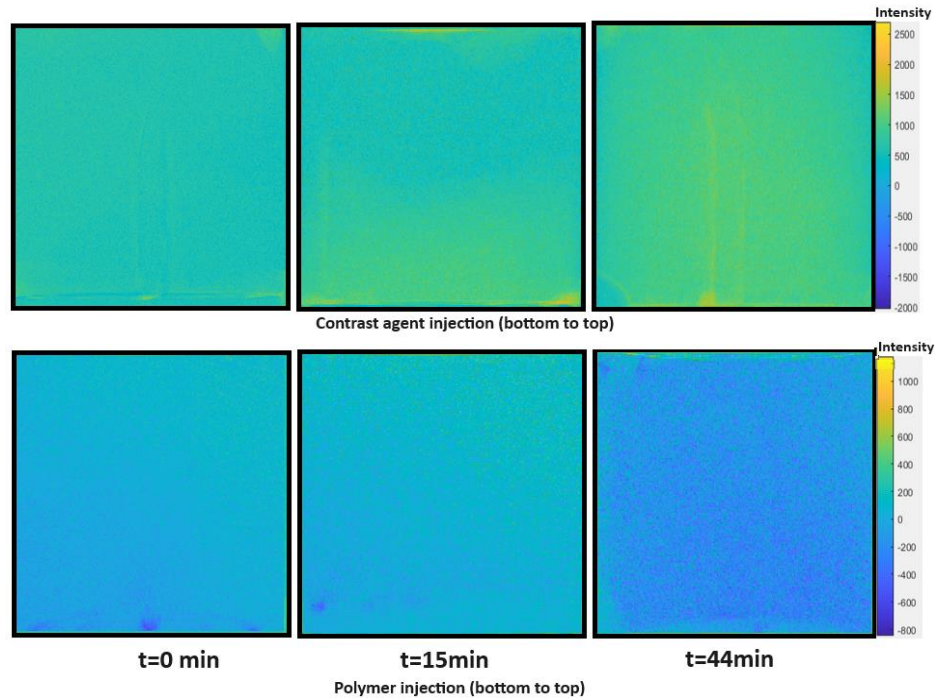


Fig. 6: Radiography images of flow and transport of the contrast agent (top row) and polymer injection (bottom row) in fractured chalk for different time intervals

Fig. 7 depicts the injection of polymer gel into the unfractured chalk formation, both before and after to the increasing the temperature to $70\text{ }^{\circ}\text{C}$ under the same pressure difference (5 atm) It is obvious that, in the process of injecting polymer at ambient temperature, the flow ($Q(\text{cc}/\text{min})$) became restricted as a result of the fouling layer of polymer molecules at the entry of the chalk, ultimately leading to blocking the flow in that region. Following the application of heat, the polymer once again exhibited a phase transition, transitioning back into a solid state. Nevertheless, after the polymer gelation period, the flow abruptly ceased and effectively obstructed the entirety of the flow pathway. Due to the chalk's limited permeability, it is possible that the polymer may not uniformly penetrate the whole core. Figure 8 depicts this process, starting with the measurement of the initial pressure drop in the chalk core during forward water flow (represented by the red line), under a consistent flow injection (indicated by the purple line). Subsequently, polymer is injected in the same direction, maintained at a steady pressure of 5 atmospheres for the duration of one pore volume. The next phase involves backward water injection, carried out in the reverse direction at the same flow rate (green line), while monitoring the pressure drop for each rate (blue line) post-polymer injection. The resultant data shows a significant increase in pressure, more than tripling from its initial value, which validates the efficacy of the polymer in obstructing the flow channels.

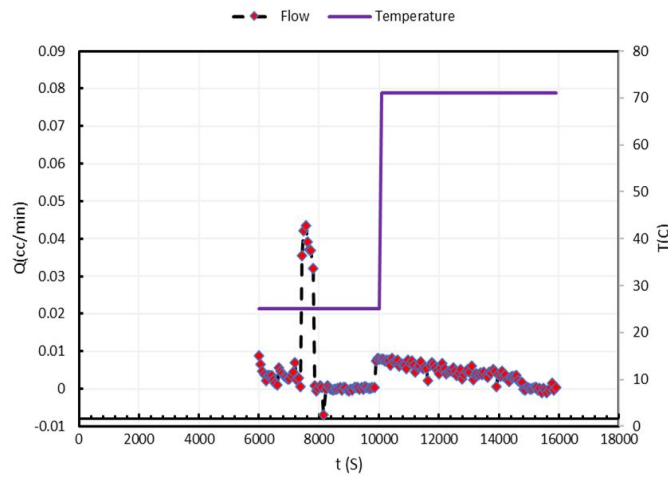


Fig. 7: Fluid flow reduction during polymer gel injection (dash line red point) before and after increasing the temperature(solid line)

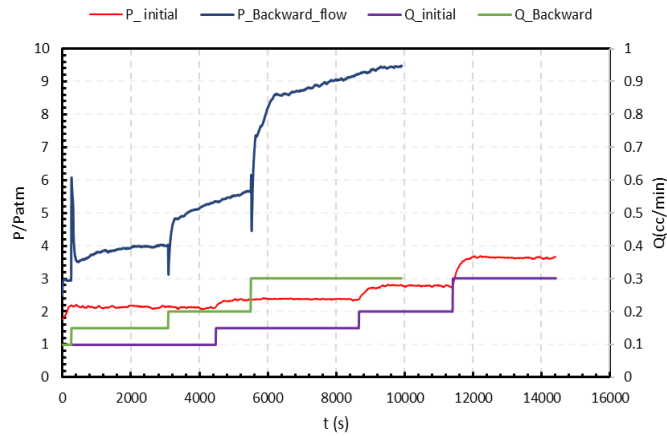


Fig. 8: Illustration of permeability assessment through reverse flow test in chalk core

4. Conclusion

In summary, this study contributes to our knowledge of efficient well sealing and abandonment tactics, specifically as they pertain to the conversion of gas and oil wells into locations for CO₂ storage. The research paper's novel methodology of employing low-viscosity polymer gels in chalk formations underscores a potentially viable substitute for conventional cement plugs, particularly in environments with restricted permeability.

The demonstration of the use of polymer gels that undergo a phase transition to high-viscosity compounds when heated, showcases an innovative approach to efficiently seal both matrix porosity and fractures in chalk formations. We also demonstrate the ability of computed tomography (CT) to monitor the anchoring process in real-time, thereby assuring efficient gelation and uniform distribution of the polymer. This methodology not only resolves the technical obstacles linked to traditional plugging techniques but also complies with environmental regulations and safety considerations.

Acknowledgements

We extend our sincere gratitude to DTU Offshore, 3D Imaging Center at DTU Physics, and the Dansk Polymer Center at DTU for graciously providing access to their laboratory facilities.

References

- [1] M. Jayachandran, R. K. Gatla, K. P. Rao, G. S. Rao, S. Mohammed, A. H. Milyani, A. A. Azhari, C. Kalaiarasy, and S. Geetha, "Challenges in achieving sustainable development goal 7: Affordable and clean energy in light of nascent technologies," *Sustainable Energy Technologies and Assessments*, vol. 53, p. 102692, 2022.
- [2] E. Trudel, M. Bizhani, M. Zare, and I. A. Frigaard, "Plug and abandonment practices and trends: A British Columbia perspective," *Journal of Petroleum Science and Engineering*, vol. 183, p. 106417, 2019.
- [3] R. Kiran, C. Teodoriu, Y. Dadmohammadi, R. Nygaard, D. Wood, M. Mokhtari, and S. Salehi, "Identification and evaluation of well integrity and causes of failure of well integrity barriers (A review)," *Journal of Natural Gas Science and Engineering*, vol. 45, pp. 511-526, 2017.
- [4] A. O. Chukwuemeka, G. Oluyemi, A. I. Mohammed, and J. Njuguna, "Plug and abandonment of oil and gas wells—A comprehensive review of regulations, practices, and related impact of materials selection," *Geoenergy Science and Engineering*, p. 211718, 2023.
- [5] T. Vrålstad, A. Saasen, E. Fjær, T. Øia, J. D. Ytrehus, and M. Khalifeh, "Plug & abandonment of offshore wells: Ensuring long-term well integrity and cost-efficiency," *Journal of Petroleum Science and Engineering*, vol. 173, pp. 478-491, 2019.
- [6] M. Khalifeh, A. Saasen, M. Khalifeh, and A. Saasen, "Tools and techniques for plug and abandonment," in *Introduction to Permanent Plug and Abandonment of Wells*, pp. 213-247, 2020.
- [7] M. Khalifeh, A. Saasen, and T. Vrålstad, "Potential utilization of geopolymers in plug and abandonment operations," in *SPE Norway Subsurface Conference*, SPE-169231, 2014.
- [8] D. Zhu, B. Bai, and J. Hou, "Polymer gel systems for water management in high-temperature petroleum reservoirs: a chemical review," *Energy & Fuels*, vol. 31, no. 12, pp. 13063-13087, 2017.
- [9] S. Lei, J. Sun, K. Lv, Q. Zhang, and J. Yang, "Types and Performances of Polymer Gels for Oil-Gas Drilling and Production: A Review," *Gels*, vol. 8, no. 6, p. 386, 2022.
- [10] D. Zhu, J. Hou, Q. Wei, and Y. Chen, "Development of a high-temperature-resistant polymer-gel system for conformance control in Jidong oil field," *SPE Reservoir Evaluation & Engineering*, vol. 22, no. 01, pp. 100-109, 2019.
- [11] H. Movahedi, S. Jamshidi, and M. Hajipour, "New insight into the filtration control of drilling fluids using a graphene-based nanocomposite under static and dynamic conditions," *ACS Sustainable Chemistry & Engineering*, vol. 9, no. 38, pp. 12844-12857, 2021.
- [12] H. Movahedi, S. Jamshidi, and M. Hajipour, "Hydrodynamic Analysis and Cake Erosion Properties of a Modified Water-Based Drilling Fluid by a Polyacrylamide/Silica Nanocomposite during Rotating-Disk Dynamic Filtration," *ACS Omega*, vol. 7, no. 48, pp. 44223-44240, 2022.
- [13] A. A. Schiefler, H. O. Sørensen, S. Bruns, D. Mütter, K. Uesugi, and D. J. Tobler, "Time resolved pore scale monitoring of nanoparticle transport in porous media using synchrotron X-ray μ -CT," *Environmental Science: Nano*, vol. 10, no. 9, pp. 2224-2231, 2023.
- [14] A. A. Schiefler, S. Bruns, D. Mütter, K. Uesugi, H. O. Sørensen, and D. J. Tobler, "Retention of sulfidated nZVI (S-nZVI) in porous media visualized by X-ray μ -CT—the relevance of pore space geometry," *Environmental Science: Nano*, vol. 9, no. 9, pp. 3439-3455, 2022.